Article

Intelligent Energy Management Control for Extended Range Electric Vehicles Based on Dynamic Programming and Neural Network

Lihe Xi [1], Xin Zhang [1,*], Chuanyang Sun [1], Zexing Wang [2], Xiaosen Hou[1] and Jibao Zhang [1]

[1] Beijing Key Laboratory of Powertrain for New Energy Vehicle, Beijing Jiaotong University, Beijing 100044, China; xilihe@bjtu.edu.cn (L.X.); 14116369@bjtu.edu.cn (C.S.); 11116345@bjtu.edu.cn (X.H.); 14116367@bjtu.edu.cn (J.Z.)

[2] Beijing Electric Vehicle Co. LTD., Beijing 102606, China; wangzexing@bjev.com.cn

* Correspondence: zhangxin@bjtu.edu.cn; Tel.: +86-(10)-5168-8404

Abstract: The extended range electric vehicle (EREV) can store much clean energy from the electric grid when it arrives at the charging station with lower battery energy. Consuming minimum gasoline during the trip is a common goal for most energy management controllers. To achieve these objectives, an intelligent energy management controller for EREV based on dynamic programming and neural networks (IEMC_NN) is proposed. The power demand split ratio between the extender and battery are optimized by DP, and the control objectives are presented as a cost function. The online controller is trained by neural networks. Three trained controllers, constructing the controller library in IEMC_NN, are obtained from training three typical lengths of the driving cycle. To determine an appropriate NN controller for different driving distance purposes, the selection module in IEMC_NN is developed based on the remaining battery energy and the driving distance to the charging station. Three simulation conditions are adopted to validate the performance of IEMC_NN. They are target driving distance information, known and unknown, changing the destination during the trip. Simulation results using these simulation conditions show that the IEMC_NN had better fuel economy than the charging deplete/charging sustain (CD/CS) algorithm. More significantly, with known driving distance information, the battery SOC controlled by IEMC_NN can just reach the lower bound as the EREV arrives at the charging station, which was also feasible when the driver changed the destination during the trip.

Keywords: energy management strategy; extended range electric vehicle; dynamic programming; neural network; state of charge

1. Introduction

Air pollution in large cities is predominantly caused by the exhaust emissions of gasoline vehicles [1]. In order to achieve the goals of low-carbon green cities, it is necessary to transform traditional fuel vehicles into new energy vehicles [2,3]. The electric vehicle plays an important role in this transition, with its advantages of no pollution or emissions. However, technical limitations, such as low battery power and short driving range, significantly affect the promotion of electric vehicles [4]. Extended range electric vehicles (EREVs) not only have the characteristics of low emissions and pollution, but also extend the endurance mileage of vehicles [5].

In conventional hybrid electric vehicles (HEVs), the battery is treated as an energy buffer. The battery state of charge (SOC) varies over a small range during the trip [6]. However, the EREV is a type of plug-in HEV, and it has a large battery for storing electric power from a charging station [7,8]. A charging cycle, which constitutes the whole life of the EREV, can be considered as the EREV leaving

a charging station with full battery energy and arriving at one charging station or another. If the EREV finishes the trip and reaches the charging station with low battery energy, it can store more clean energy from the grid. Then, the fuel consumption of the extender can be reduced on the next trip for the same total energy demand [9,10].

In the past, two control strategies were used to realize the aforementioned control goals. They were the charging deplete/charging sustain (CD/CS) strategy and the blended control strategy [11–13]. According to the former strategy, vehicles work in a pure electric mode within the all-electric range (AER), and this stage is called the CD stage [14] Beyond the AER, the extender is turned on as the main energy source to satisfy the average power demand from the traction motor (TM). The battery works in coordination with the extender during higher power demands, such as fast acceleration or on an upslope, and the battery SOC is maintained over a small range around the lower bound; this stage is called the CS stage [15]. Banvait et al. proposed an intelligent CD/CS strategy for a plug-in hybrid electric vehicles (HEVs) [16,17]. After restricting the engine working area under the CD and CS modes, the velocity, power demand and current battery SOC were used as control variables to determine the extender turn on/off time and output power value. However, the battery SOC dropped to the low threshold before the vehicle arrived at the charging station, which meant that the battery energy conversion efficiency was poor; therefore, this strategy was not an optimal control method. Schacht et al. proposed an EREV energy management strategy in which the equivalent consumption minimization strategy (ECMS) was applied during the CS mode [18]. The equivalent factor (EF), which is the ratio of electric power and fuel consumption, has a significant influence on the working state of the extender. Determining the appropriate EF for different driving cycles requires a considerable amount of effort, which has limited the application of this strategy.

For the blended strategy, the extender works in coordination with the battery to provide electrical energy for the TM from the beginning of the trip. The battery SOC drops slowly to the lower bound [19]. Phillip et al. designed a blended strategy based on the rule-based control method [20]. This control strategy compares the power demand and the lower threshold of the engine output power to determine the extender turn on/off and its output power range. Chen et al. proposed a multimode control strategy in which control rules were extracted from dynamic programming (DP) optimization results [21]. Since the EREV is a highly nonlinear system, sometimes the control rules cannot be extracted conveniently for different vehicle performances and configuration parameters, and they are not suitable for all HEV systems. In [22–24], an intelligent energy management system (EMS) was proposed based on DP and NN. Since the proposed method trained the optimal setting for a settled driving cycle, the generated controller was not applicable for driving cycles with other driving distances.

Although the CD/CS strategy is simple to implement for real-time control, its fuel economy is poorer than that of the blended strategy [25]. This is because the extender provides the average power demand for the TM in the CS mode, and the engine in the extender works in the low efficiency region. Moreover, secondary energy conversion in the EREV dynamic system reduces the system's efficiency. Karbowski et al. pointed out that battery energy losses can be reduced when a lower SOC is achieved only at the end of a trip [26]. Therefore, a controller capable of the following is necessary for the EREV: (1) adjusting the battery SOC to the lower bound as the EREV arrives at a charging station; (2) reducing the working duration when the battery is in the lower energy state; and (3) decreasing the fuel consumption during the trip.

To achieve this goal, an intelligent energy management controller based on DP and NN (IEMC_NN) is proposed in this study. The IEMC_NN consists of four parts: the NN controller module library; the target battery SOC calculation module; electricity consumption per unit distance, E_{per}, calculation module; and the NN controller selection module. The module library includes three NN controllers to emulate the optimal results, which were optimized by the DP. The selection module estimates the future optimal E_{per} consumed by the EREV and selects the appropriate NN controller, which determines the extender turn on/off time and output power value. Three driving conditions was applied to validate the performance of the IEMC_NN: unknown driving distance, atypical driving

distance and target driving distance changes during the trip. It was shown that the proposed controller could achieve the control objectives above and improve the fuel economy by 10–28% compared with the CD/CS strategy.

The remainder of this paper is organized as follows. Section 2 shows the EREV energy management optimization problem formulation and a comprehensive description of DP. The NN is described in Section 3. Section 4 presents the IEMC_NN framework. Simulation results are shown in Section 5. Finally, the conclusions are presented in Section 6.

2. Optimization Problem and Formulation

The energy management problem can be described as a dynamic optimization problem, which can be generally expressed by the following equation [27]:

$$x(k+1) = f(x(k), u(k)) \tag{1}$$

where $x(k)$ represents the state variable, such as vehicle velocity and battery SOC, and $u(k)$ represents the control variable, which can be represented by battery current and extender output power. When the state of the EREV system is $x(k)$ at step k, using the action of control variable $u(k)$, the vehicle system can be transformed to the next state $x(k+1)$ at step $k+1$. The energy optimization of the EREV can be formulated as follows:

$$\min_{\overline{u}} J(\overline{x}, \overline{u}) \text{ subject to } C(\overline{x}, \overline{u}) \leq 0 \tag{2}$$

where $J(\overline{x}, \overline{u})$ is the cost-to-go function and $C(\overline{x}, \overline{u}) \leq 0$ are the constraints on the variables. The energy optimization problem for the EREV is solved by the DP algorithm, and our goal is to minimize the cost function over a given driving cycle. First, the vehicle powertrain and subsystem models were constructed before applying the DP algorithm.

2.1. EREV Configuration

The EREV powertrain model considered in this study is schematically shown in Figure 1. The black line represents the mechanical connection. The lines with arrows represent the electrical connection, and the arrows point in the power flow direction. $P_{ex,elec}$, $P_{m,elec}$ and $P_{b,elec}$ represent extender output power, traction motor power and battery electric power, respectively. The parameters of the main components are listed in Table 1. All the parameters are from an ongoing project.
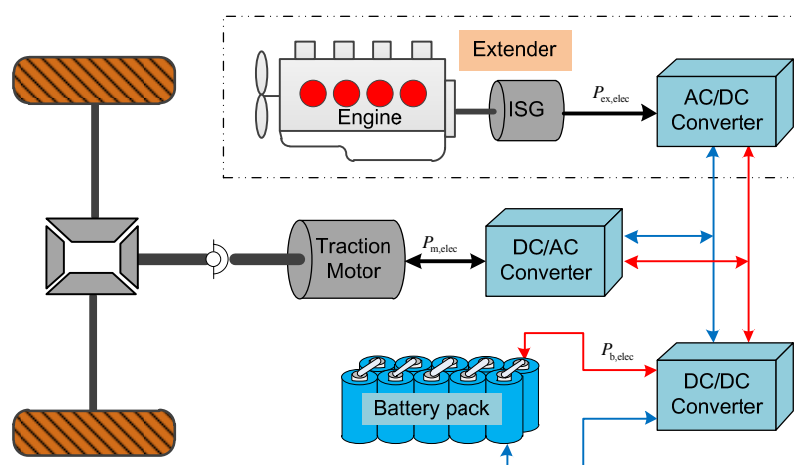

Figure 1. Extended range electric vehicle (EREV) powertrain configuration and power flow.

Table 1. EREV component parameters.

Components	Parameters	Values
Engine	Displacement/L	0.9
	Maximum power/kW	52
	Maximum torque/Nm	90
Generator	Maximum power/kW	53
	Maximum torque/Nm	155
Traction motor	Maximum power/kW	130
	Maximum torque/Nm	480
Power Battery	Capacity/Ah	37
	Voltage/V	360
Others	Final drive ratio	7.793
	Curb mass/kg	1400
	Front area/m^2	2.9
	Tire rolling radius/m	0.298
	Transmission efficiency/%	92

2.2. EREV Subsystem Model

Considering that the DP process relies on the state transition equations of the EREV, a complex vehicle model with a large number of states is not suitable, because a heavy computational load will emerge. Thus, a simplified dynamic model for the vehicle, extender and battery was developed.

(1) Vehicle model:

In this study, the vehicle is modeled as a mass-point moving in the longitudinal direction. The traction motor required power P_{req}, which can be determined through Equation (3) [28].

$$P_{\mathrm{req}} = \frac{v}{\eta_t} \left(\frac{\delta M}{3600} \frac{\mathrm{d}v}{\mathrm{d}t} + \frac{Mgf\cos\alpha}{3600} + \frac{C_D A}{76140} v^2 + \frac{Mg\sin\alpha}{3600} \right) \tag{3}$$

where δ represents the mass factor that equivalently converts the rotational inertias of the rotating components into translational mass; M represents the vehicle gross weight; v represents the vehicle velocity; f represents the rolling resistance coefficient; η_t represents the transmission efficiency; a represents the road gradient; C_D represents the aerodynamic drag coefficient; and A represents the vehicle frontal area.

(2) Extender model:

The extender is a system that consists of an engine and a generator. With no mechanical connection to the traction motor, the extender can be operated independently at the maximum efficiency line, which is formed by a series of points. The maximum efficiency line is obtained from the extender efficiency map, which is a combination of the maps of the engine and generator. In this study, the extender transient influence is eliminated, and the fuel consumption of the engine in the extender is determined by its static operating points. The maximum efficiency line of the extender system is shown in Figure 2. Once the extender's output power is determined, the fuel consumption can be obtained by the following equation:

$$\dot{m}_{\mathrm{fuel}} = f(P_{\mathrm{ex}}) \tag{4}$$

where $\dot{m}_{\mathrm{fuel}}$ represents the fuel consumption rate and P_{ex} represents the electric power generated by the extender. $f(P_{\mathrm{ex}})$ describes the relationship between the output power of the extender and the fuel consumption rate.
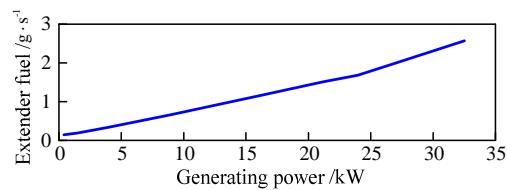
Figure 2. Extender output power vs. fuel consumption rate.

(3) Battery model:

The R_{int} model is adopted as the battery model, which is simplified as an equivalent circuit with an open voltage source and a resistance. The rate of change of the SOC can be calculated by using the following equation:

$$\frac{\text{dSOC}}{\text{d}t} = \frac{v_{oc} - \sqrt{v_{oc}^2 - 4R_{int}(P_{req} - P_{ex})}}{2R_{int}Q_b} \tag{5}$$

where v_{oc} represents the battery open-circuit voltage and R_{int} represents the battery internal resistance, which is obtained from two look-up tables (charging/discharging). P_{req} represents the power demand of the TM motor, and it is positive when driving and negative when braking; and Q_b represents the battery capacity.

2.3. Dynamic Programming

One of the control objectives in this study is to consume minimum gasoline and electricity. To achieve these goals, there are different control requirements for the battery and extender during the trip, which are as follows:

For the battery: (1) the vehicle should avoid working for a long time when the battery is in the low energy state, because the high internal resistance of the battery will result in a large heat loss; (2) the more battery energy that is released as the EREV arrives at the charging station, the more electric energy from the grid will be stored in the battery for the next trip.

For the extender: If the remaining driving distance from the charging station is beyond the AER, the extender provides additional electric energy for TM with minimum gasoline consumption.

The control objectives above can be interpreted as a cost function or constraint in DP, and appropriate variables are also necessary. The extender output power and battery SOC have an inherent relationship based on Equation (5). Therefore, the battery SOC and the extender output power were selected as the state variable and the control variable, respectively. To decrease the vehicle working duration when the battery was in the low SOC state, the difference between the current battery SOC and target SOC was presented in the cost function. The fuel consumption rate was also included in the cost function, which is expressed as follows:

$$\begin{cases} J = \displaystyle\sum_{k=0}^{N-1} L(x(k), u(k)) \\ L(x(k), u(k)) = \alpha \cdot \dot{m}_{fuel}(k) + \beta \cdot |SOC(k) - SOC_{des}(k)| \end{cases} \tag{6}$$

where $L(x(k), u(k))$ represent the instantaneous cost function; $SOC(k)$ is the current battery SOC; and $SOC_{des}(k)$ is the target battery SOC value, which can be defined as follows:

$$\text{SOC}_{des}(k) = (\text{SOC}_{init} - \text{dis}_{cur}(k) \frac{\text{SOC}_{init} - \text{SOC}_{final}}{\text{dis}_{all}}) \tag{7}$$

where dis_{all} represents the target driving length. It describes the distance between the EREV starting point and the charging station, where the EREV finishes its trip; $\text{dis}_{cur}(k)$ represents the current driving

length; SOC_{init} represents the initial battery SOC when at the start of the trip; and SOC_{final} represents the final SOC as the EREV arrives at the charging station.

The battery SOC target curve is shown in Figure 3. The EREV stores a sufficient amount of electric energy in the battery at the initial location. Three driving distances, named S_1, S_2 and S_3, were assumed to stand for different driving purposes or charging station locations. Each final battery SOC is the lower bound according to the control objectives. Thus, the battery target SOC for each driving distance is AB, AC and AD, based on Equation (7).
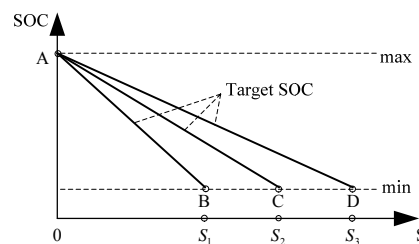
Figure 3. Battery target SOC for different target driving distances.

In order to ensure safe and smooth operation of the extender and battery during the optimization process, the following physical constraints need to be satisfied:

$$\begin{cases} SOC_{min} \leq SOC\,(k) \leq SOC_{max} \\ P_{chg,max} \leq P_b\,(k) \leq P_{dis,max} \\ P_{ex,min} \leq P_{ex}\,(k) \leq P_{ex,max} \\ P_{delt\_ex,min} \leq P_{delt\_ex}\,(k) \leq P_{delt\_ex,max} \\ T_{e,min} \leq T_e\,(k) \leq T_{e,max} \\ \omega_{ex,min} \leq \omega_{ex}\,(k) \leq \omega_{ex,max} \end{cases} \tag{8}$$

where SOC_{min} and SOC_{max} represent the lower and upper bounds of the battery SOC, respectively; $P_{chg,max}$ and $P_{dis,max}$ represent the power limits for battery discharging and charging, respectively; and $P_{ex,min}$ and $P_{ex,max}$ represent the lower and upper constraints of APU output power, respectively. P_{delt_ex} represents the change rate of the extender output power; $T_{e,min}$ and $T_{e,max}$ represent the lower and upper bounds of the engine torque, respectively; and $\omega_{ex,min}$ and $\omega_{ex,max}$ represent the lower and upper constraints of the extender speed, respectively.

Since the battery SOC changes slowly, the sampling time for the EREV control problem is selected as 1 s. Based on Bellman's principle, the DP algorithm is a multi-step decision process, which decomposes the optimization problem into a sequence of smaller minimization problems that can be solved recursively [29,30]. Subsequently, the algorithm finds the sequence of the optimal extender output power $P_{ex}(k)$ values that minimize the cost function over the entire drive cycle while satisfying all constraints, as shown in Equation (8).

The sub-problems for each step are expressed as follows:

For the *N*-th step (final time step):

$$J_N^*\,(x(N)) = \min_{u(N)} [L\,(x\,(N)\,,u\,(N))] \tag{9}$$

For the *k*-th ($1 \leq k \leq N-1$) step:

$$J^*\,(x(k)) = \min_{u(k)} [L\,(x\,(k)\,,u\,(k)) + J^*\,(x(k+1))] \tag{10}$$

Here, $J^*(x(k))$ represents the optimal cost-to-go function from state $x(k)$ at time k to the final time and $L(x(k), u(k))$ represents the one-step cost when the EREV system takes an action $u(k)$ at the given state $x(k)$ that results in a future state $x(k + 1)$.

With the nonlinear system of the extender and battery, the state variable *SOC*(k) does not fall on the grid points precisely, and the cost-to-go value of $J^*(x(k))$ and $L(x(k), u(k))$ are determined through linear interpolation [31].

3. Neural Network Learning Optimal Control

The DP optimization of the EREV system assumes that detailed trip information is known a priori. However, the actual future driving speed can hardly be known in advance [32]. Moreover, it also requires prohibitive computer memory and results in large computational time; thus, the DP optimization approach cannot be applied directly to an online energy management problem [33]. The NN algorithm can effectively solve the nonlinear system problem. It can learn the optimized results and generate an online controller for optimal energy distribution [34]. A multilayered multiclass NN was developed, as shown in Figure 4. The input layer had six nodes representing power demand, velocity, current SOC, target SOC, driving mode (including driving, braking and parking) and SOC error. The output node represented extender output power. The trained controller could be used by the vehicle control unit (VCU) to generate the extender's turn on/off time and its output power.
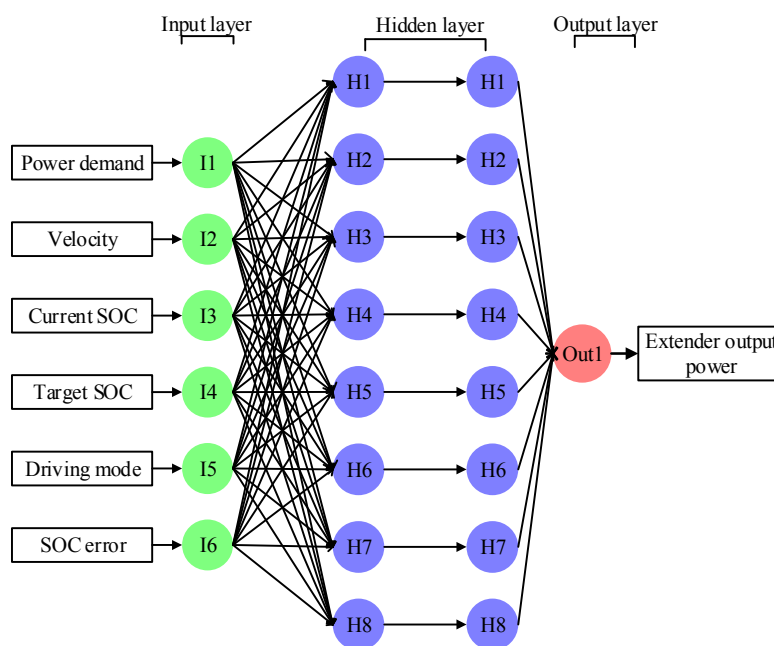

Figure 4. Neural network diagram.

The well-known back-propagation algorithm was adopted to train the NN. The training and test data were obtained from the DP optimization results. The NN's training performance was measured by the method of mean squared errors (MSEs):

$$MSE = \frac{1}{N} \sum_{k=1}^{N} (output(k) - tar(k))^2 \tag{11}$$

where $output(k)$ is the NN output and $tar(k)$ are the target data. The training target MSE is 0.001.

Because several interpolations were used to calculate the cost function during DP, the generated training and test data had a higher numerical precision. However, the data transmitted via the CAN bus did not have the same level of precision. Before applying the NN framework to train the optimal

setting, the precision of each node training data was adjusted according to transmission accuracy of the CAN bus data, which is listed in Table 2.

Table 2. Training data accuracy settings.

Layer	Parameters	Accuracy
Input layer	Power demand/kw	0.1
	Velocity/km·h^{-1}	0.01
	Current SOC/%	0.1
	Target SOC/%	0.1
	SOC error/%	0.1
	Driving trend	1
Output layer	Extender output power/kw	0.1

The detailed design and application procedure used to train the controller based on DP and NN for EREVs are illustrated in Figure 5. The process mainly consisted of five parts: standard driving cycles were repeated several times to construct simulation driving cycles with different target driving distances; the power demand array for the simulation driving cycle was generated from the powertrain model; the DP algorithm was applied to iteratively optimize the power split ratio between the extender and battery for the driving cycle; the NN was adopted to learn the distribution setting obtained from the DP and to generate the NN controller; and the trained NN controller was used to build an online energy management controller. The detailed operation for each part has been described in the previous sections.
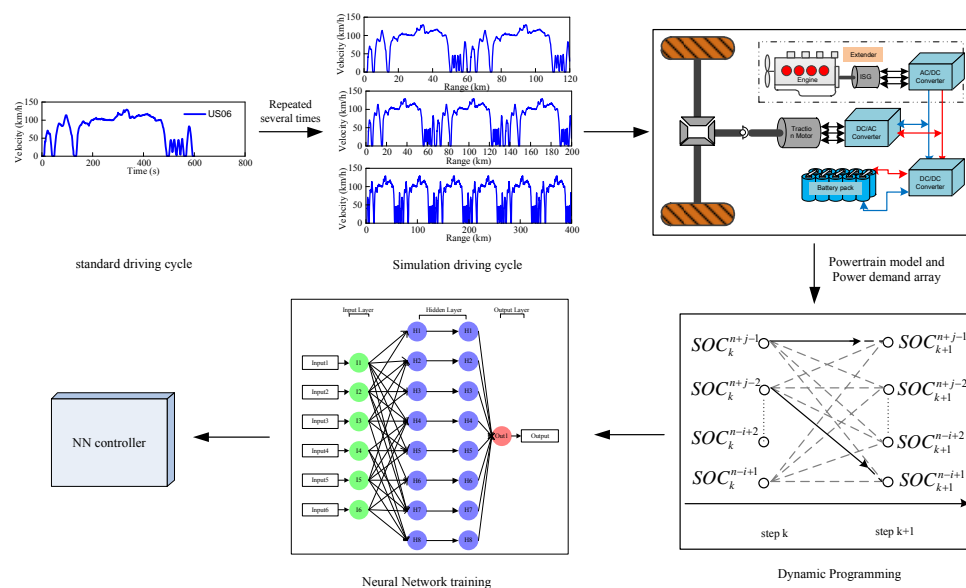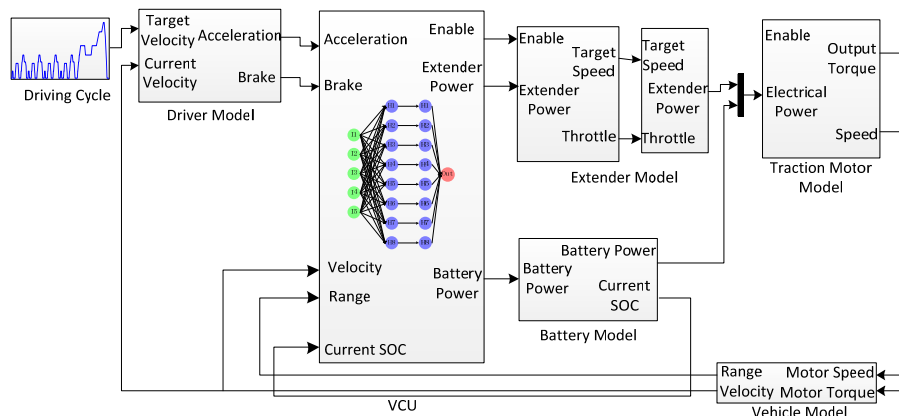

Figure 5. NN controller design diagram.

Figure 6 shows the generated NN controller's performance and regression during neural network training, and it can be seen that the trained NN controller can emulate the optimal extender output power from the DP results well. In order to confirm that the trained NN controller could achieve the optimal energy allocation generated by DP further, a forward simulation platform was built in MATLAB/Simulink, as can be seen in Figure 7. The simulation platform consisted of a driver model, a vehicle control unit, an extender model, a traction model and a longitudinal vehicle dynamics model. Since the RC model could express the battery dynamics with high accuracy, it was adopted as the battery model. In addition, as the battery's working behavior is considerably affected by temperature, a thermal model was added to compensate for any such effects.
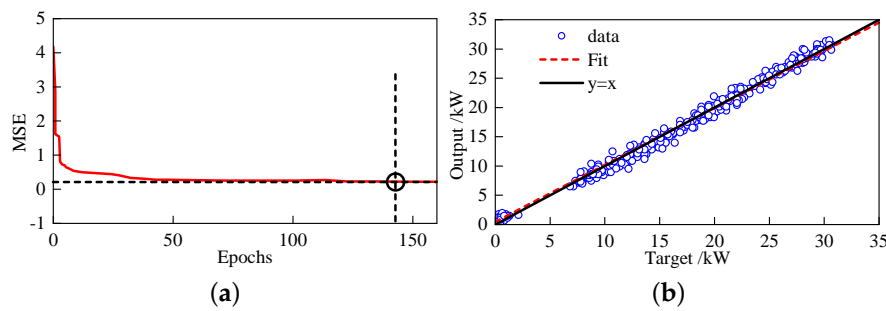
Figure 6. Neural network training performance and regression. (**a**) Mean squared errors vs. epochs; (**b**) the regression between training data and output.

Figure 7. NN controller design diagram.

The New Europe Driving Cycle (NEDC) was used to construct a 120-km simulation driving cycle, which is adopted to validate the trained NN controller performance. The DP optimization results and the NN controller simulation results are compared in Figure 8. The battery SOC and extender output power are shown in Figure 8a,b, respectively. Their differences are shown in Figure 8c,d. It can be observed that the extender output power values generated from the NN controller were very close to the DP results, indicating that the NN controller had a better performance in learning the DP behavior.
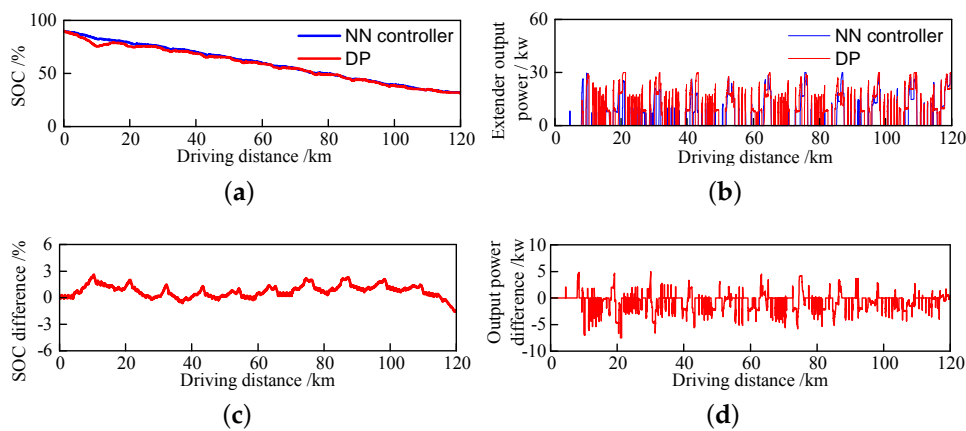
Figure 8. Comparison between DP and NN controller results under the 120-km NEDC cycle. (**a**) Battery SOC variation; (**b**) extender output power comparison; (**c**) battery SOC difference; (**d**) extender output power difference.

4. Intelligent Online Control

The NN controller in Section 3 was also applied to the NEDC driving cycle with lengths of 80-km and 165-km. The simulation results are shown in Figure 9. For the 80-km driving cycle, the battery SOC dropped to nearly 50% when the vehicle reached its destination. In this case, 20% of the available electric energy was stored in the battery, which limited the recharge ability. For the 165-km driving cycle, the battery SOC dropped to 30% as the EREV arrived at the 120-km mark, and then, the vehicle was operated in a charge-sustaining mode until the end of the trip; this is the protection method for the battery. It can be concluded that the NN controller trained from one driving cycle is not suitable for cycles with other driving distances because the parameter target SOC in the cost-function has an inherent relationship with the driving distance; in other words, there is only one target SOC curve for a particular driving distance. Training NN controllers for each driving distance can solve the problem; however, this will require additional effort. Moreover, it is not feasible to download such a large number of trained controllers into the controller hardware. Therefore, an intelligent energy management controller based on several NN controllers (IEMC_NN) was designed to solve this problem.
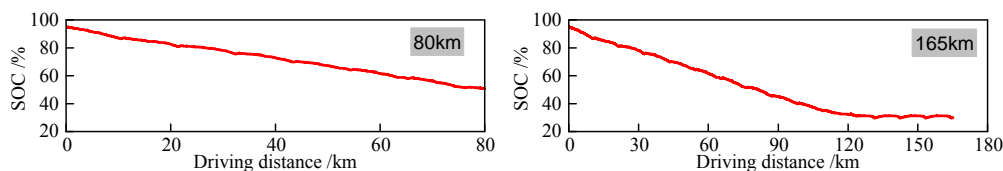

Figure 9. Battery SOC variations of the 120-km NN controller under different driving distances.

Figure 10 shows the proposed IEMC_NN operation flowchart. It contains four modules: the NN controller module library; the target battery SOC calculation module based on Equation (7); the electricity consumption per unit distance, E_{per}, calculation module; and the NN controller selection module. The primary idea of IEMC_NN is to intelligently select an appropriate NN controller from the controller module library for different driving distances. The detailed operation for each part will discussed in the following sections.
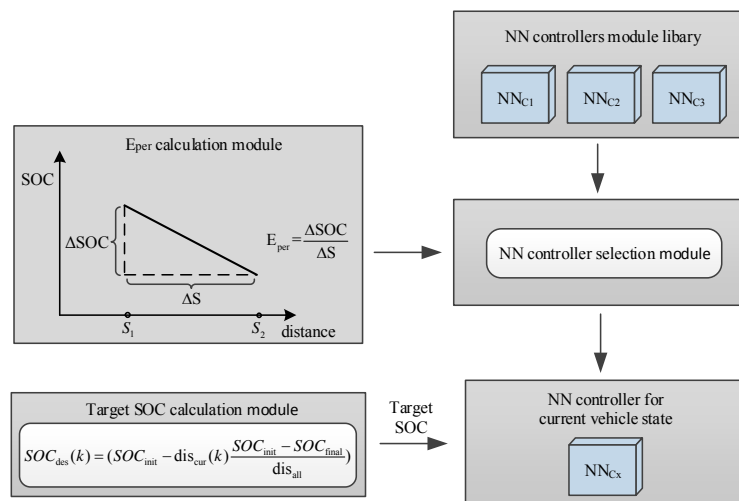

Figure 10. Detailed operation flowchart of intelligent energy management controller for EREV based on dynamic programming and neural networks (IEMC_NN).

4.1. Controller Module Library

The controller module library is built based on the generated NN controllers, which are trained from typical driving distances. The typical driving distance can be determined through the analysis that follows. According to the report in [35], the average daily driving distance for a driver in China is approximately 40 km. Owing to the charging time cost and inadequate charging equipment nowadays, a plug-in HEV driver may go to a charging station every couple of days. In this study, the driver goes to charging station every three days with low battery energy. Under this assumption, the EREV leaves the charging station with full battery energy, and after traveling approximately 120 km, the vehicle reaches the charging station again. Thus, one of the typical driving distances is 120 km. In addition, the extended range of the EREV under the NEDC cycle is 400 km, which is adopted as the typical long driving distance. The length of the medium driving distance is set as 200 km. Therefore, the typical driving distances in this study are 120 km, 200 km and 400 km. Then, three NN controllers are generated from the training driving cycle with typical driving distances based on the method described in Section 3; those controllers are named as NN_{C1}, NN_{C2} and NN_{C3}.

4.2. Intelligent Energy Management Controller

4.2.1. Electricity Consumption per Unit Distance Calculation Model

The extender can be turned on/off properly to adjust the battery SOC varying along the target curve according to the available battery energy and remaining range. The electricity consumption per unit distance, E_{per}, is defined to quantify the relationship between the available battery capacity and the remaining range.

$$E_{per} = \Delta SOC / \Delta S = (SOC_{cur}(k) - SOC_{final}) / (dis_{all} - dis_{cur}(k)), \tag{12}$$

where ΔSOC represents the available battery capacity; ΔS represents the remaining range from the current location to the end of the trip; $SOC_{cur}(k)$ is the current battery SOC; SOC_{final} represents the final battery SOC as the EREV arrives at the charging station (30% in this study).

The trained NN controller can control battery SOC variations along the target curve, and thus, the current battery SOC, $SOC_{cur}(k)$, can be replaced by the target battery SOC, $SOC_{des}(k)$. Combined with Equation (7), Equation (12) can be modified as follows:

$$E_{per} = (SOC_{init} - SOC_{final}) / dis_{all} \tag{13}$$

In this study, the EREV leaves the charging station with full battery energy; when it arrives at the charging station the next time, the battery energy is used up. Thus, the initial and final battery SOC are constant values in Equation (13), and E_{per} is only related to the driving distance for an EREV.

4.2.2. NN_Controller Selection Module

Since a linear relationship exists between the target SOC and driving distance, the future E_{per} value generated by an NN controller is fixed. Thus, an appropriate NN controller can be selected based on estimating an ideal future E_{per} value consumed by the EREV to regulate the trajectory of the battery SOC.

The E_{per} consumed by NN_{C1}, NN_{C2} and NN_{C3} is defined as E_{per_120}, E_{per_200} and E_{per_400}, respectively. A diagram showing the operation of the controller selection module in IEMC_NN is shown in Figure 11. The detailed control rules are described as follows:

(1) When the IEMC_NN cannot obtain driving distance information after the vehicle leaves the charging station, it assumes that the EREV has arrived at the charging station after driving about 120 km. In this case, the IEMC_NN will adopt the NN_{C1} controller.

(2) When the EREV with full battery energy leaves the charging station and the target driving distance is shorter than AER, the EREV will be operated in the charging depleted mode

(3) When the target driving distance is a typical driving distance, i.e., 120, 200 or 400 km, NN_{C1}, NN_{C2} or NN_{C3} will be applied in the IEMC_NN for the corresponding driving distance.

(4) In most cases, the target driving distance is not the typical driving distance; such a distance is called the untrained driving distance. In this case, the trained controller cannot be applied directly. The selection module in the IEMC_NN can intelligently employ an appropriate NN controller. Its operating method is illustrated in Figure 12. The destination location is set at 165 km in this case, and the EREV is fully charged at the initial location.

First, the selection module determines that the target driving distance is between 120 km and 200 km. Then, the NN_{C2} controller is adopted in IEMC_NN at the beginning of the trip. The battery SOC will vary along the target line AC, and the battery will not reach its low threshold as the EREV arrives at Point E. This is because one NN controller leads to one E_{per} being consumed by the EREV. Changing the NN controller during the trip can adjust the battery SOC trajectory. When the battery SOC varies to Point B, the future E_{per} becomes E_{per_120}; NN_{C1} is employed instead of NN_{C2}; and then, the battery SOC varies along target curve BE.

(5) If the battery SOC reaches the low threshold before the vehicle arrives at the charging station, the EREV will be operated in the charging sustain mode to protect the battery life.
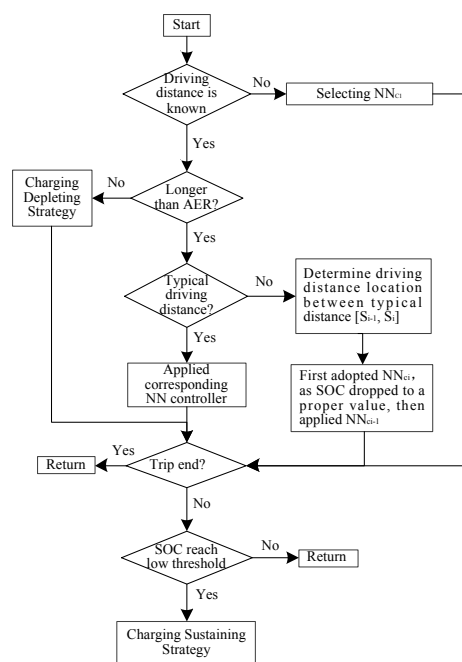

Figure 11. Flowchart of the operation of the controller selection module in IEMC_NN.
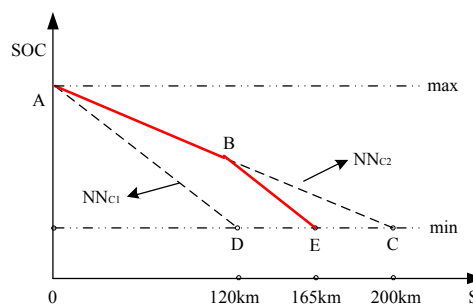

Figure 12. Battery SOC variation for an atypical driving distance to illustrate the selection methods in IEMC_NN.

5. Simulation Results and Analysis

According to the description of the IEMC_NN in Section 4, the IEMC_NN can intelligently select an NN controller based on the target driving distance information. To validate the controller performance, three categories of target driving distances were tested: unknown driving distance, atypical driving distance and changing target driving distance during the trip.

5.1. Simulation with Unknown Driving Distance

Suppose that the IEMC_NN cannot obtain the target driving distance information after leaving the charging station. The LA92 driving cycle was applied to validate the IEMC_NN performance with unknown driving distance

The length of a single LA92 driving cycle was 15.8 km. It was repeated 10-times to construct a simulation cycle with a total length of 158 km. The beginning SOC was 95%. The CD/CS controller was also applied to this cycle as a comparison. The simulation results are shown in Figure 13.
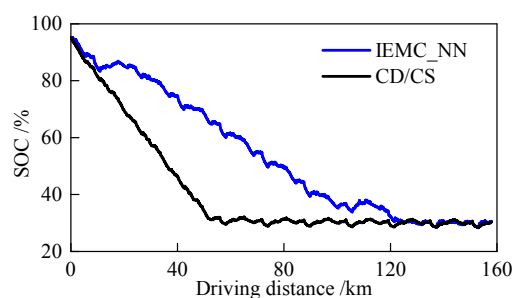

Figure 13. Battery SOC comparison for the condition of driving distance information unknown (LA92 cycle). CD/CS, charging deplete/charging sustain.

The IEMC_NN controller battery SOC slowly decreased to 30% as the EREV passed the 120-km mark. The E_{per} consumed in this phase was close to E_{per_120}. Thus, it was inferred that NN_{C1} was applied at the beginning of the route. Then, the battery SOC maintained a certain level until the EREV reached its destination. For the CD/CS controller, the battery SOC reached 30% as the EREV achieved a distance of 60 km, and then, the vehicle worked in CS mode until the end of the trip. The fuel economies of these two control methods were compared and are shown in Table 3. The comparison shows that, although the target driving distance information was not available, the IEMC_NN controller improved fuel economy by 28.6% when compared to the CD/CS controller.

Table 3. Fuel economy comparison for the unknown driving distance information condition (LA92 cycle).

| Controller	Duration/s	Target Driving Distance/km	Fuel Consumption/L	Final SOC/%	Saving Rate/%
CD/CS	14360	158	6.36	30.5	-
IEMC_NN	14360	158	4.54	30.5	28.6

Figure 14 shows a comparison of the engine working point distribution corresponding to the IEMC_NN and CD/CS controller. It can be seen that the engine operates close to the optimal efficiency curve when the IEMC_NN controller is applied. In other words, the proposed controller realizes better fuel economy than the CD/CS controller. For the IEMC_NN controller, since the extender working point has been optimized by the DP algorithm, the engine was operated closer to the optimal efficiency curve than that of the CD/CS controller. Since the CD/CS controller started extender, to follow the power demand as battery SOC in the low energy state, the extender working point of the CD/CS controller was distributed in the whole region of the engine consumption map. This way, it can prove that the proposed IEMC_NN controller improved the fuel economy.
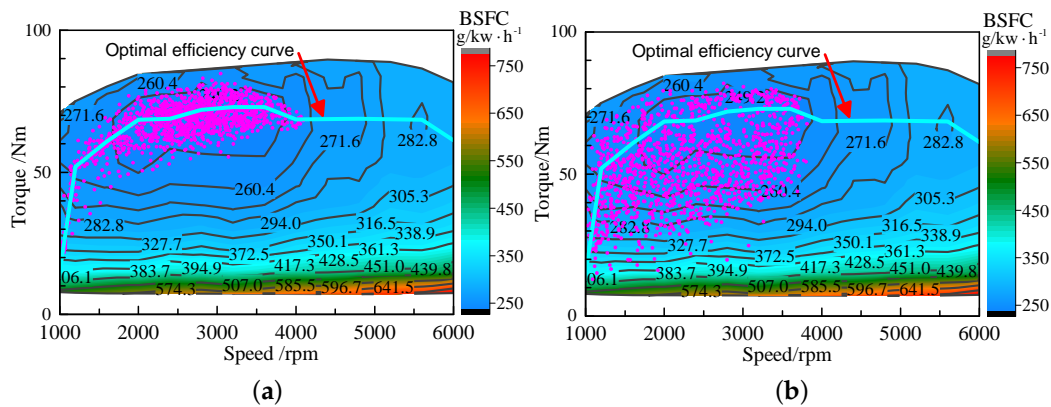
Figure 14. Engine working point comparison. (**a**) IEMC_NN engine working points; (**b**) CD/CS engine working points.

5.2. Simulation with a Normal Driving Distance

In most cases, the target driving distance was not a typical driving distance, and the IEMC_NN was still feasible for these cases based on the existing trained NN controllers. To evaluate the controller for this case, the NEDC driving cycle was used to construct a simulation cycle with a total distance of 165 km. Three control methods, namely, IEMC_NN, NN_{C1} controller only and CD/CS controller, were compared under this driving cycle. Their simulation results are shown in Figure 15.
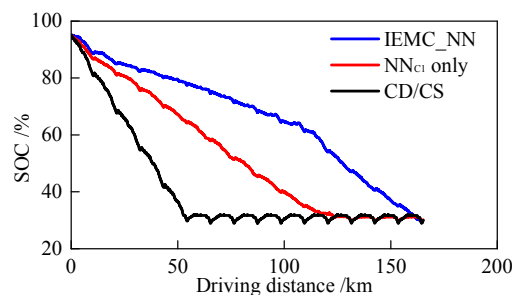
Figure 15. Battery SOC variation under a normal driving distance (NEDC, 165 km).

The simulation results show the battery SOC trajectory can be divided into two stages for the IEMC_NN. In the first stage, the battery SOC changed slowly and decreased to 60.6% when the EREV was driven for approximately 114 km. According to Equation (13), the E_{per} consumed in this stage was very close to E_{per_200}; therefore, the NN_{C2} controller was applied during this stage. Then, the battery SOC decreased quickly and reached a low threshold as the EREV completed the trip. The value of E_{per} in the second stage was almost E_{per_120}. This result is attributed to the NN_{C1} controller. Unlike other controllers, the proposed controller, IEMC_NN, can use up the battery energy exactly as the EREV completes the trip.

Table 4 shows a comparison of the fuel economy values for the three controllers. The fuel consumptions for the three controllers CD/CS, NN_{c1} only and IEMC_NN were 5.22 L, 4.87 L and 4.77 L, respectively, and their final SOC values were 29.5%, 30.2% and 31.5%, respectively. However, the final SOC of the IEMC_NN was slightly higher than the low threshold of 30%; hence, the equivalent fuel consumption calculation method was adopted for fair comparison [36]. The IEMC_NN improved the fuel saving rate by 10.2% when compared to the CD/CS controller and by 3.5% when compared to the NN_{C1} controller.

Thus, when the target driving distance was not a typical driving distance, the IEMC_NN controller not only adjusted the battery SOC, reducing it to a low threshold as the EREV finished the trip, but also increased fuel economy.

Table 4. Comparison of untrained driving distance fuel economy (NEDC cycle).

Controller	Duration/s	Target Driving Distance/km	Fuel Consumption/L	Final SOC/%	Saving Rate/%
CD/CS	17699	165	5.22	29.5	-
NN$_{C1}$ only	17699	165	4.87	30.2	6.7
IEMC_NN	17699	165	4.77	31.5	10.2

5.3. Simulation with a Changing Target Driving Distance during the Trip

Sometimes, the target driving distance changes during the trip. If the VCU cannot adjust in a timely manner, the battery SOC may not reduce to the low threshold as the EREV arrives at the charging station. The HWFET driving cycle was repeated 10-times to construct a simulation cycle with the length of 165 km. Now, consider that the first target driving distance of the driver is 120 km when the EREV covers a distance of 25 km, but the driver then changes the target driving distance to 165 km. Three control methods were tested. In one method, the NN$_{C1}$ controller remained unchanged; in another, the IEMC_NN was applied to adjust the controller intelligently, and in the last method, the CD/CS algorithm was applied. The simulation results are shown in Figure 16.

According to the above-mentioned assumption, when the battery SOC decreases up to Point A (25 km, 79%), the driver changes the target driving distance to 165 km instead of 120 km. In the first control method, the NN$_{C1}$ controller was applied without any adjustments, and the descending trend of the battery SOC remained unchanged before the vehicle reached point C (120 km, 30%). However, the EREV had not finished the trip yet, and the vehicle worked in the charging sustain mode, in which the SOC was varied around 30% until the vehicle completed the trip. For the IEMC_NN, the initial target driving distance was 120 km; therefore, the NN$_{C1}$ controller was selected, and the trajectory of the battery SOC coincided exactly with that of the first control method. When the battery SOC reached Point B (47.1 km, 67.3%), the trajectory trend changed, and Point D (165 km, 30%) was attained, as the EREV arrived at the end point of the trip. The SOC trajectory BD is parallel to the NN$_{C2}$ target curve.
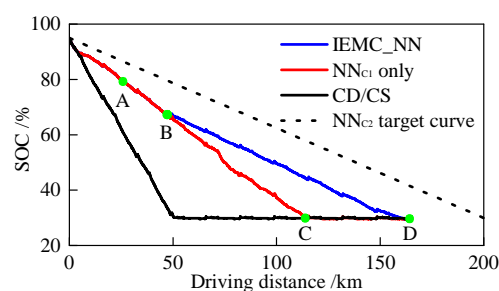

Figure 16. Battery SOC comparison when the target driving distance changes during the trip (HWFET cycle).

A comparison of the fuel economies of the two control methods is presented in Table 5. It can be seen that the proposed controller can adjust the NN controller in time as the driver changes the destination and improve the fuel economy by approximately 13.3%. Further, it is seen that reducing the EREV working time as the battery enters the low energy state can improve fuel economy.

The equivalent economy improvements for the IEMC_NN and CD/CS controller are shown in Figure 17. All the improvement results were determined through the equivalent fuel consumption calculation method. The results indicate that the proposed controller, IEMC_NN, improved the economy by about 10–28% when compared to the CD/CS controller.

Table 5. Fuel economy comparison when the target driving distance changes during the trip (HWFET cycle).

Controller	Duration/s	Target Driving Distance/km	Fuel Consumption/L	Final SOC/%	Saving Rate/%
CD/CS	7660	165 km	7.29	30.5	-
NN_{C1} only	7660	165 km	6.86	30.5	5.9
IEMC_NN	7660	165 km	6.32	30.0	13.3
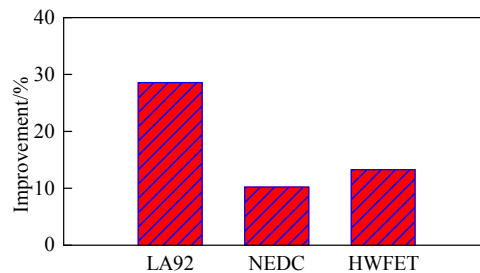
Figure 17. Fuel economy improvements for the IEMC_NN controller compared to the CD/CS controller.

6. Conclusions

This study focuses on designing an energy management controller, which can control battery SOC close to the lower bound as the EREV arrives at the charging station and which can improve the EREV's storage of more clean energy from the electric grid. Meanwhile, consuming minimum gasoline during the trip is another design target. An intelligent energy management controller for EREV, namely, IEMC_NN, was proposed to achieve the goals above. The control objectives were presented as cost function, and DP was applied to obtain the optimal split ratio between the extender and battery. A neural network has been designed and trained to generate the NN controller, which was adopted to control battery SOC variation by emulating the optimal extender power. Simulation results show that the error between the SOC controlled by the trained NN controller and target SOC is within 3%. Three typical driving distance were selected based on the driving statistics, and the corresponding trained NN controllers, named as NNC1, NN C2 and NN C3, constructed the controller module in IEMC_NN. The other components in IEMCS were the electricity consumption per unit distance (E_{per}) calculation module, the target battery SOC calculation module and the NN controller selection module.

Three conditions were simulated to validate the performance of the IEMC_NN: unknown driving distance, atypical driving distance and target driving distance changing during the trip. Comparing the simulation results between IEMC_NN and the CD/CS controller, the following conclusions could be drawn:

(1) If the driving distance to the charging station is known, the IEMC_NN can intelligently select the NN controller depending on the remaining battery energy and the driving distance to the charging station. The battery SOC can just drop to the lower bound as the EREV reaches the charging station, and the vehicle's working duration as the battery is in a low energy state can be minimized. Simulation results show that IEMC_NN improves the fuel saving rate by 10.2% compared to the CD/CS controller under the NEDC cycle. Even if the target driving distance changes during the trip, the IEMC_NN can still be feasible, and the fuel economy can be improved by 13.3% under the HWFET cycle.

(2) If the driving distance is unknown, the IEMC_NN adjusts the battery SOC varying along the default target curves and the terminal SOC close to the lower bound. Compared to the CD/CS controller, the IEMC_NN can improve fuel economy by approximately 28.6% under the LA92 cycle.

In this study, the IEMC_NN performance has been only validated by simulation. The slope of the road, which can influence the driveline power, is not considered in IEMC_NN. Moreover, the service life of the battery and extender are also neglected. A more comprehensive work, considering the influence

factors above, will be carried out to improve the performance of IEMC_NN, and an experiment by a real application will be adopted to validate the controller.

Author Contributions: Lihe Xi and Xin Zhang mainly proposed the energy managment strategy and optimal approach. Chuanyang Sun and Zexing Wang built up the simulation model and helped to program the algorithm. All the authors, included Xiaosen Hou and Jiabao Zhang, did the simulation analysis, results discussions, and contributed to the paper writing work.

Conflicts of Interest: The authors declare no conflict of interest.

References

1. Shi, X.Q.; Sun, Z.X.; Li, X.; Li, J.; Yang, J. A comparative study on environmental impacts of life cycle between electric taxi and fuel taxi in Beijing. *Environ. Sci.* **2015**, *36*, 1105–1116.

2. Chen, Z.; Xiong, R.; Wang, K.; Jiao, B. Optimal energy management strategy of a plug-in hybrid electric vehicle based on a particle swarm optimization algorithm. *Energies* **2015**, *8*, 3661–3678.

3. Un-Noor, F.; Sanjeevikumar, P.; Mihet-Popa, L.; Mollah, M.N.; Hossain, E. A Comprehensive study of key electric vehicle (EV) components, technologies, challenges, impacts, and future direction of development. *Energies* **2017**, *10*, 1217.

4. Gu, Q.; Dou, F.; Ma, F. Energy optimal path planning of electric vehicle based on improved A* algorithm. *Trans. Chin. Soc. Agric. Mach.* **2015**, *46*, 316–322.

5. Hall, J.; Marlok, H.; Bassett, H.; Warth, M. Analysis of real world data from a range extended electric vehicle demonstrator. *SAE Int. J. Altern. Power.* **2015**, *4*, 20–33.

6. Hong, S.; Wenjie, L.; Jing-Min, Y.; Yin-Ping, G. Optimization of energy management strategy for a Paralle-l series HEV. *Trans. Chin. Soc. Agric. Mach.* **2009**, *40*, 31–35.

7. Fraidl, G.K.; Beste, F.; Kapus, P.E.; Korman, M.; Sifferlinger, B.; Vincen, B. Challenges and solutions for range extenders—From concept considerations to practical experiences. In Proceedings of the TO ZEV—Highlighting the Latest Powertrain, Vehicle and Infomobility Technologies, Turin, Italy, 9–10 June 2011.

8. Škugor, B.; Cipek, M.; Deur, J. Control variables optimization and feedback control strategy design for the blended operating regime of an extended range electric vehicle. *SAE Int. J. Altern. Power.* **2014**, *3*, 152–162.

9. Song, W.; Zhang, X.; Tian, Y.; Xi, L. Driving pattern recognition and charging management-based intelligent control strategy for extended-range electric vehicles. *J. Automot. Safety Energy* **2016**, *7*, 224–229.

10. Song, W.; Zhang, X.; Tian, Y.; Xi, L. A charging management-based intelligent control strategy for extended-range electric vehicles. *J. Zhejiang Univ. Sci. A (Appl. Phys. Eng.)* **2016**, *17*, 903–910.

11. Wirasingha, S.G.; Emadi, A. Classification and review of control strategies for plug-in hybrid electric vehicles. In Proceedings of the Vehicle Power and Propulsion Conference (VPPC '09), 7–10 September 2009, Dearborn, MI, USA; pp. 907–914.

12. Du, J.; Chen, J.; Song, Z.; Gao, M.; Ouyang, M. Design method of a power management strategy for variable battery capacities range-extended electric vehicles to improve energy efficiency and cost-effectiveness. *Energy* **2017**, *121*, 32–42.

13. Xie, S.; Li, H.; Xin, Z.; Liu, T.; Wei, L. A pontryagin minimum principle-based adaptive equivalent consumption minimum strategy for a plug-in hybrid electric bus on a fixed route. *Energies* **2017**, *10*, 1379.

14. Patil, R.; Adornato, B.; Filipi, Z. Design optimization of a series plug-in hybrid electric vehicle for real-world driving conditions. *SAE Int. J. Engines* **2010**, *3*, 655–665.

15. Hai-tao, M.; Dong-jin, Y.; Yuan-bin, Y. Optimization of the control strategy for range extended electric vehicle. *Automot. Eng.* **2014**, *36*, 899–903.

16. Banvait, H.; Anwar, S.; Chen, Y. A rule-based energy management strategy for plug-in hybrid electric vehicle (PHEV). In Proceedings of the American Control Conference (ACC'09), St. Louis, MO, USA, 10–12 June 2009; pp. 3938–3943.

17. Rousseau, A.; Pagerit, S.; Gao, D.W. Plug-in hybrid electric vehicle control strategy parameter optimization. *J. Asian Electr. Veh.* **2008**, *6*, 1125–1133.

18. Schacht, E.; Bezaire, B.; Cooley, B.; Bayar, K.; Kruckenberg, J.W. Addressing drivability in an extended range electric vehicle running an equivalent consumption minimization strategy. In Proceeding of the SAE 2011 World Congress & Exhibition, Detroit, MI, USA, 12–14 August 2011.

19. Waldner, J.; Wise, J.; Crawford, C.; Dong, Z. Development and testing of an advanced extended range electric vehicle. In Proceeding of the SAE 2011 World Congress & Exhibition, Detroit, MI, USA, 12–14 August 2011.

20. Sharer, P.B.; Rousseau, A.; Karbowski, D.; Pagerit, S. *Plug-in Hybrid Electric Vehicle Control Strategy: Comparison between EV and Charge-Depleting Options*; SAE Technical Paper 2008-01-0460; SAE International: Warrendale, PA, USA; Troy, MI, USA, 2008.

21. Chen, B.C.; Wu, Y.Y.; Tsai, H.C. Design and analysis of power management strategy for range extended electric vehicle using dynamic programming. *Appl. Energy* **2014**, *113*, 1764–1774.

22. Chen, Z.; Mi, C.C.; Xu, J.; Gong, X.; You, C. Energy management for a power-split plug-in hybrid electric vehicle based on dynamic programming and neural networks. *IEEE Trans. Veh. Technol.* **2014**, 63, 1567–1580.

23. Murphey, Y.L.; Park, J.; Chen, Z.; Kuang, M.L.; Masrur, M.A.; Phillips, A.M. Intelligent hybrid vehicle power control—Part I: Machine learning of optimal vehicle power. *IEEE Trans. Veh. Technol.* **2012**, *61*, 3519–3530.

24. Murphey, Y.L.; Park, J.; Chen, Z.; Kuang, M.L.; Masrur, M.A.; Phillips, A.M. Intelligent hybrid vehicle power control—Part II: Online intelligent energy management. *IEEE Trans. Veh. Technol.* **2013**, *62*, 69–79.

25. Zhou, W.; Zhang, C.; Li, J. Analysis and comparison of optimal power management strategies for a series plug-in hybrid school bus via dynamic programming. *INT. J. Vehicle. Des.* **2015**, *69*, 113–131.

26. Karbowski, D.; Rousseau, A.; Pagerit, S.; Sharer, P. Plug-in vehicle control strategy: From global optimization to real-time application. In Proceedings of the 22nd electric vehicle symposium, EVS22, Yokohama, Japan, 25 October 2006.

27. Patil, R.M.; Filipi, Z.; Fathy, H.K. Comparison of supervisory control strategies for series plug-in hybrid electric vehicle powertrains through dynamic programming. *IEEE Trans. Contr. Syst. Technol.* **2014**, *22*, 502–509.

28. Yu, Z. *Automobile Theory*; China Machine Press: Beijing, China, 2009.

29. Bellman, R.E.; Dreyfus, S.E. *Applied Dynamic Programming*; Princeton University Press: Princeton, NJ, USA, 1962.

30. Sundström, O.; Ambühl, D.; Guzzella, L. On implementation of dynamic programming for optimal control problems with final state constraints. *Oil Gas Sci. Technol.* **2009**, *65*, 91–102.

31. Wang, X.; He, H.; Sun, F.; Zhang, J. Application study on the dynamic programming algorithm for energy management of plug-in hybrid electric vehicles. *Energies* **2015**, *8*, 3225–3244.

32. Zou, Y.; Hou, S.; Han, E.; Liu, L.; Chen, R. Dynamic programming-based energy management strategy optimization for hybrid electric commercial vehicle. *Automot. Eng.* **2012**, *34*, 663–668.

33. Lin, C.C.; Peng, H.; Jeon, S.; Jang, M.L. Control of a hybrid electric truck based on driving pattern recognition. In Proceedings of the 2002 Advanced Vehicle Control Conference, Hiro Shima, Japan, 9–13 September 2002; pp. 41–58.

34. Park, J.; Chen, Z.; Kiliaris, L.; Kuang, M.L.; Masrur, M.A.; Phillips, A.M.; Murphey, Y.L. Intelligent vehicle power control based on machine learning of optimal control parameters and prediction of road type and traffic congestion. *IEEE Trans. Veh. Technol.* **2009**, *58*, 4741–4756.

35. Beijing Daily. *Using Intensity Too High Need to Be Guided*; Tong Xin Press: Beijing, China, 2011.

36. Niu, J.; Si, L.; Zhou, S.; Zhang, T. Simulation analysis of energy control strategy for an extended-range electric vehicle. *J. Shanghai Jiaotong Univ.* **2014**, *48*, 140–145.